Article citation info:
Bouaouiche K, Menasria Y, Khalifa D. Bearing fault detection using a method involving absolute value spectrum and impulsivity evaluation. Diagnostyka. 2024;25(2):2024213. https://doi.org/10.29354/diag/188371.

DIAGNOSTYKA, 2024, Vol. 25, No. 2

e-ISSN 2449-5220
DOI: 10.29354/diag/188371

BEARING FAULT DETECTION USING A METHOD INVOLVING ABSOLUTE VALUE SPECTRUM AND IMPULSIVITY EVALUATION

Karim BOUAOUICHE [*], **Yamina MENASRIA**, **Dalila KHALFA**

[1] Electromechanical Engineering Laboratory, Badji Mokhtar University, Annaba, Algeria
[*] Corresponding author, e-mail: karimbouaouiche@gmail.com

Abstract

This study analyzes vibration signals related to bearing defects using a method that reconstructs an effective signal. This reconstruction is based on the determination of the instantaneous amplitude and phase. Then, a decomposition method is applied to the amplitude and phase to obtain several simple functions. Once the functions are obtained, an evaluation of impulsivity is performed on each function using the proposed parameter. This selects functions that contain fault data. The important signal is then identified and used. After the creation of the effective signal, filtering by a morphological operator with a structuring element is applied to improve the signal quality. Finally, in the spectrum of the absolute values of this signal, the defect can be detected from the frequency of the peaks. Signals from different databases were analyzed using the proposed method, illustrating the results in the form of high-amplitude peaks in the frequency of bearing component defects.

Keywords: amplitude value spectrum, defect detection, bearing, impulsivity evaluation

List of Symbols/Acronyms

AHDE– Dilation and erosion average-hat operator;
AHCO– Closing and opening average-hat operator;
a – Contact angle;
AI– Instantaneous amplitude;
an – Analytic signal;
CWRU–Case Western Reserve University;
Dm– Pitch diameter;
d– Ball diameter;
EMD – Empirical Mode Decomposition;
EFD – Empirical Fourier Decomposition;
F – Function;
Fr –Operating speed;
F_{or}– Fault frequency of the outer ring;
$\bar{F}(\omega)$– Fourier spectrum magnitudes;
f_n– Frequencies;
f_s– Sampling frequency;
f_c– Characteristic fault frequency;
GI – Gini index;
H – Hilbert transform;
HI – Hoyer index;
Im– Imaginary part;
Ku– Kurtosis;
L–Signal length;
L_{SE}–Length of the structural element;
MHPO1– Morphology hat product operation;
MCKD– Maximum Correlated Kurtosis Deconvolution;
NE– Negentropy;
P– Parameter;
QI– Instantaneous phase;
R– Real part;
SVMD – Successive Variational Mode Decomposition;
SE– Structuring Element;
$u(\omega)$– Band-pass filters;
$x(t)$– Vibration signal;
$\bar{x}$ – Mean;
$\|\vec{x}\|_1$– L1 norm;
$X(\omega)$– Spectrum of the signal;
z– Number of balls.

1. INTRODUCTION

Bearings are components consisting of an inner and outer ring, a cage, and a rolling element. They are generally used as links between shafts for transmitting motion and supporting loads. In the event of poor operating conditions, the bearings can fail, leading to partial or total machine failure. According to statistics, bearings are responsible for between 40% and 45% of faults in rotating machines [1], making them a strategic component. Several diagnostic and prognostic techniques are used to detect defects. These include acoustic analysis based on the analysis of acoustic emission signals [2]. Similarly, ultrasonic analysis enables the detection of defects on the basis of the transmission and reception of an ultrasonic wave through the material [2]. Moreover, vibration analysis focuses on monitoring abnormal vibrations produced by defects, whereas thermography analysis relies on defect detection based on variations in thermodynamic properties [2]. However, vibration

Received 2023-12-03; Accepted 2024-05-07; Available online 2024-05-27

analysis is more feasible for fault monitoring and detection because it offers several signal processing methods [3]. Fault detection using vibration signal analysis consists of two essential steps [4]. The first step involves the collection of signals by a measurement chain comprising acceleration, speed, or displacement sensors [4]. The second step involves processing the signals using a specific diagnostic method [4]. Signal analysis is performed in three domains: the time domain, where the signal varies as a function of time; the frequency domain, which shows the variation of vibration amplitude as a function of frequency; and the time–frequency domain, which illustrates the signal as a function of both time and frequency [4].

The analysis of vibration signals in the time domain is performed using statistical indicators to assess the bearing condition, such as the statistical parameter known as kurtosis, created by D. Dyer et al. [5]. This parameter takes a value lower than three for a healthy bearing with a Gaussian distribution of vibration amplitude [5]. Many statistical indicators are used in the field of defect detection, such as the Gini index of economic origin [6]. However, it is applied in the processing of vibration signals to evaluate the pulses produced by the defect [6]. This index is more efficient than kurtosis [6]. In addition, the L2/L1 norm proposed by Jia et al. [7], the Hoyer index used by Zhao et al. [8], and negative entropy exists. Entropy, a thermodynamic concept, is used to identify the complexity of systems, but negative entropy is a parameter used in the same context as other parameters for assessing signal impulsivity [9]. In addition, the generalized logarithm penalty strengthens the signal pulses while reducing noise, demonstrating increased efficiency [10]. The complexity of signals offers additional insight for detecting faults, such as the weighted entropy index, which can be used to select disordered and ordered signals [11]. Disordered signals containing complex data with several pulses are not similar to sinusoidal signals [11]. Furthermore, comparing data from the bearing's healthy state with that of its current state makes it easy to detect faults without locating faulty components in the bearing [12].

Frequency signal analysis is based on the representation of the signal's vibration amplitude as a function of frequency, using transformations such as the Fourier transform to obtain the spectrum and the Hilbert transform, which are widely used for signal envelope analysis [13]. Time–frequency analysis is performed using transformations such as the Hilbert–Huang transform [13]. This transform is a combination of the Hilbert transform and the signal decomposition method known as empirical mode decomposition (EMD) [13]. Empirical mode decomposition is the first method of signal decomposition proposed by Huang et al. [14]. Over time, several decomposition methods have been used in the diagnosis of bearing defects, such as the SVMD method developed by Nazari et al. [15]. Noise, poor positioning and mounting of the sensor result in the measurement of a low-quality noisy signal [16]. To ensure noise suppression, it is necessary to apply certain methods such as morphological operators and band pass filtering around the resonance frequency [16]. The two pass frequencies of this filter are usually represented by a kurtogram, which represents the variation of the spectral kurtosis as a function of the frequency [12]. In addition, deconvolution methods are widely applied to extract the impulse portion of the signals, which contains defect information [16].

Artificial intelligence, which consists of machine learning and deep learning, opens a new path in the field of machine fault diagnosis. In general, the principle of diagnosis using artificial intelligence consists in extracting the defect characteristics from the signal and then introducing them into a classification model, such as the one proposed by Sun.Y et al., which involve transforming the signal into a symmetric image used as the input parameter for the convolution neural network [17]. Therefore, depending on the performance of the classifier, the efficiency of the diagnostic method can be assessed as being better or not. To this end, several performance improvement techniques have been developed, such as the probabilistic impulse response model with a multi-layer structure proposed by Zuo.L et al., to improve the impulse neural network [18]. The features used in the classification model, such as vector support machines, can be determined from the variation of the signal either in the time or frequency domain, and its characteristics include statistical parameters such as mean and energy [19].

In this paper, we present a method for detecting bearing defects based on vibration signal analysis. The rest of the article is organized as follows: section (2) presents the proposed method, which integrates several signal processing tools. Sections (3 and 4) illustrates the application and evaluation of the performance of the proposed method using signal processing available in databases.

2. METHODS

We propose a method for the analysis of bearing vibration signals to detect defects. The proposed method comprises three steps, as shown in the flowchart (Fig. 1).

Step 1: Determine the instantaneous amplitude and phase using the analytical signal obtained from the Hilbert transform. The equations below express the amplitude and phase of the signal [20].

$$H[x(t)] = x(t) * \frac{1}{\pi t} \tag{1}$$

$$an(t) = x(t) + jH[x(t)] \tag{2}$$

$$AI(t) = \sqrt{x(t)^2 + H[x(t)]^2} \tag{3}$$

$$QI(t) = arctan\left(\frac{H[x(t)]}{x(t)}\right) \tag{4}$$

$$an(t) = AI[cos\ (QI) + jsin(QI)] \tag{5}$$

The following equations express the real and imaginary parts of the analytic signal [20]:

$$R(t) = x(t) = AI(t)cos\ (QI(t)) \quad (6)$$

$$Im(t) = AI(t)jsin(QI(t)) \quad (7)$$

The vibration signal is equal to the real part of the analytic signal, as shown in Eq. (6).

Once the instantaneous amplitude and phase are obtained, the EFD method is applied to break them down into several functions (F).

Empirical Fourier decomposition allows the decomposition of a signal into multiple components (F), as shown in the following steps [21]:

- Determining the spectrum of the signal to be decomposed using the Fourier transform.

$$X(\omega) = \int_{-\infty}^{+\infty} x(t)e^{-j\omega t}dt \quad (8)$$

- The separation limit of the spectrum is defined as follows:

If: $0 \le n \le N$ and $f_n \ne f_{n+1}$

$$\omega_n = arg\ \min \bar{F}(\omega) \quad (9)$$

If: $0 \le n \le N$ and $f_n = f_{n+1}$

$$\omega_n = f_n \quad (10)$$

- The construction of band-pass filters $u(\omega)$ is performed for each segmentation with a cut-off frequency (ω_n, ω_{n-1}).

$$u(\omega) = \begin{cases} 1 & if\ \omega_{n-1} \le |\omega| \le \omega_n \\ 0 & else \end{cases} \quad (11)$$

- The filtered signals, denoted as $X_n(\omega)$, originate from the decomposition of the signal to be decomposed.

$$X_n(\omega) = u(\omega)X(\omega) \quad (12)$$

$$X_n(\omega) = \begin{cases} X(\omega) & if\ \omega_{n-1} \le |\omega| \le \omega_n \\ 0 & else \end{cases} \quad (13)$$

- The decomposed components in the time domain are obtained by applying the inverse Fourier transform.

$$F_n(t) = \int_{-\infty}^{+\infty} X_n(\omega)e^{j\omega t}d\omega \quad (14)$$

- The sum of all the components allows for the reconstruction of the signal.

$$x(t) = \sum_{n=1}^{N} F_n(t) \quad (15)$$

Step 2: Assess the impulsivity of functions (F) using statistical parameters. Kurtosis is a parameter defined by Eq. (16) [12].

$$Ku = \frac{\frac{1}{L}\sum_{i=1}^{L}(x_i - \bar{x})^4}{\left(\frac{1}{L}\sum_{i=1}^{L}(x_i - \bar{x})^2\right)^2} \quad (16)$$

For a healthy bearing, kurtosis is less than three, whereas for a failing bearing, kurtosis is greater than three [5]. Negentropy, Hoyer index, Gini index, and L2/L1 norm are used to assess the impulses of the fault signal, which are defined by the following equations:

- L2/L1 norm [22]:

$$L2/L1 = \frac{\sqrt{\sum_{i=1}^{L} x_i}}{\sum_{i=1}^{L}|x_i|} \quad (17)$$

- Hoyer index (HI) [22]:

$$HI = \frac{\sqrt{L} - \frac{\sum_{i=1}^{L}|x_i|}{\sum_{i=1}^{L} x_i^2}}{\sqrt{L} - 1} \quad (18)$$

- Negentropy (NE) [23]:

$$NE = \frac{1}{L}\sum_{i=1}^{L}\left[\frac{x_i^2}{\bar{x}} ln\left(\frac{x_i^2}{\bar{x}}\right)\right] \quad (19)$$

- Gini index (GI) [6]:

$$GI = 1 - 2\sum_{i=1}^{L}\frac{x_i}{\|\vec{x}\|_1}\left(\frac{L - i + 0.5}{L}\right) \quad (20)$$

On the basis of parameter thresholds, we can determine whether the bearing is failing or healthy, as in the case of Kurtosis. However, the thresholds for the Hoyer index, Gini index, negentropy, and L2/L1 norm are unknown. Thus, we define the threshold values from the vibration signals of healthy bearings available in the CWRU database. The signals used are shown in Table (1) [24].

Table 1. 6205-SKF bearing signals

Speed [rpm]	Load [Nm/s]	Signals	Signal symbol
1730	2206.47	100.mat	S4
1750	1470.98	99.mat	S3
1772	735.49	98.mat	S2
1797	0	97.mat	S1

Depending on the values of the parameters in Table (2), several thresholds differ in defining the bearing state. In this case, we propose a parameter (P) that is considered to be the product of all statistical parameters used to evaluate signal impulsivity. Parameter (P) enables the definition of a threshold and ensures the elimination of differences between parameters, as shown in the following equation:

$$P = Ku \times L2/L1 \times NE \times GI \times HI \quad (21)$$

Table 2. Parameter values of a healthy bearing

Signals	S4	S3	S2	S1
Kurtosis	2.8658	2.7609	2.8066	2.8228
Negentropy	0.7078	0.6805	0.6948	0.7069
L2/L1 norm	1.2469	1.2369	1.2429	1.2478
Hoyer index	0.1999	0.1933	0.1972	0.2004
Gini index	0.4109	0.4036	0.4084	0.4126
Parameter (P)	0.2077	0.1812	0.1951	0.2058

According to the threshold of parameter (P), the bearing state can be defined as follows:

$$P_{threshold} = 1.25 \times max\ (P) = 0.25 \quad (22)$$

$$\begin{cases} if\ P \le 0.25 & healthy\ bearing \\ if\ P > 0.25 & faulty\ bearing \end{cases} \quad (23)$$

The new vibration signal, which contains fault information, is formulated as follows:

$$\begin{cases} AI_n(t) = \sum F_{AI}(t) \\ QI_n(t) = \sum F_{QI}(t) \end{cases} \quad P > 0.25 \quad (24)$$

$$x(t) = AI_n(t) \times cos\ (QI_n(t)) \quad (25)$$

Step 3: Noise suppression by signal filtering using the MHPO1 morphological operator developed by B.Chen et al. [25].

$$MHPO1(n) = AHDE(n) \times AHCO(n) \quad (26)$$

However, in this operation, we use a flat structuring element because it is very useful for

analyzing vibration signals and is simple. The length of a structuring element must satisfy the following condition [26]:

$$L_{SE} < \frac{f_s}{f_c} \tag{27}$$

The flat structuring element consists of zeros with a flat shape of zero height and specific length [27]. Equation (28) expresses the flat element in terms of scale (n) and length, which is equal to (n+2) [27].

$$\begin{cases} SE_i = 0 \quad i = 1,2,\dots(n+2) \\ SE = \{SE_1, SE_2, \dots, SE_{n+2}\} \end{cases} \tag{28}$$

In this step, the length of the structuring element used is equal to 12 on a scale of 5.

Instead of using the Hilbert transform or the Teager–Kaiser energy operator as the final step in the method to demodulate the signal, determine the envelope spectrum, and then detect the fault, we develop the absolute value spectrum to identify faults by comparing theoretical fault frequencies with peak frequencies in the spectrum. The absolute value spectrum is defined as follows:

$$x(f) = \int_{-\infty}^{+\infty} |x(t)| e^{-j2f\pi t} dt \tag{29}$$

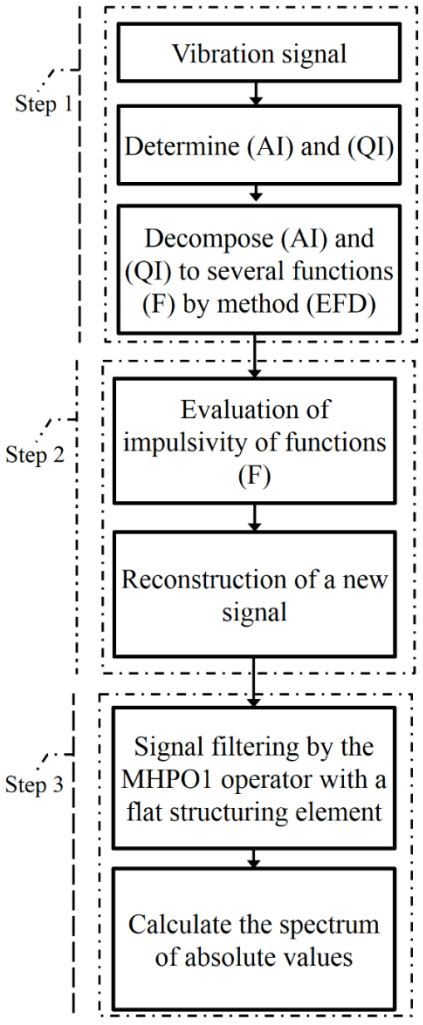

Fig. 1. Proposed method

3. EXPERIMENTAL STUDY

3.1. CWRU database

The CWRU database presents bearing vibration signal measurements from a test strip comprising an electric motor with two bearings [24]. One bearing is positioned on the driver side with a type 6205-SKF, and the other is positioned on the fan side with a type 6203-SKF [24]. Bearing vibration signals were collected using accelerometers mounted on bearing housings and recorded as MATLAB files [24]. Fault frequencies were calculated for each bearing component by multiplying the rotational speed in hertz (Hz) by the coefficients shown in Table 3 [24].

Table 3. Component coefficients

Components	6203-SKF	6205-SKF
Inner race	4.9469	5.4152
Outer race	3.0530	3.5848
Cage	0.3817	0.39828
Ball	3.9874	4.7135

To evaluate the effectiveness of the proposed method, we analyzed two vibration signals, one dependent on bearing 6205 and the other linked to bearing 6203. The characteristics of the signals are shown in Table (4) [24].

Table 4. Vibration signals

Bearing	6203-SKF	6205-SKF
Speed and Load	1730 RPM 2237.1 Nm/s	1750 RPM 1491.4 Nm/s
Defect diameter	0.1778 mm	0.1778 mm
Fault frequency	142.63 Hz	157.94 Hz
Sampling frequency	12 kHz	48 kHz
Component	Inner race	Inner race

3.1.1. Results and discussions

Case 1: Signal from the 6205-SKF bearing

The amplitude (AI) and phase (QI) of the signal are shown in Figure 2. For the EFD method, the decomposition level is four, and the amplitude (AI) and phase (QI) functions are shown in Figures (3) and (4).

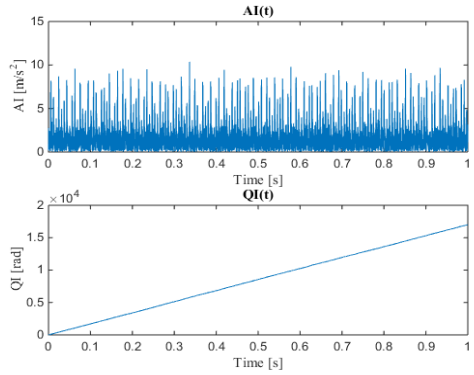

Fig. 2. Amplitude and phase

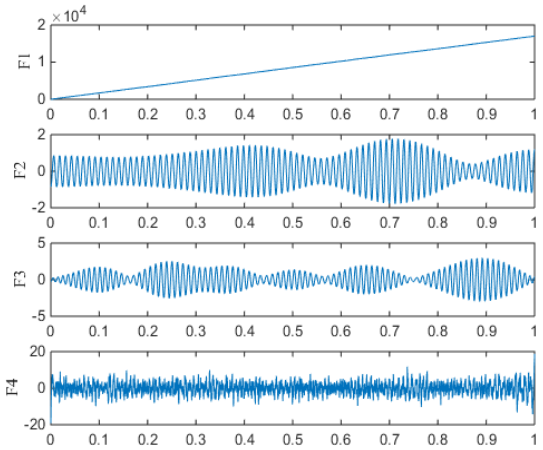

Fig. 3. Phase functions

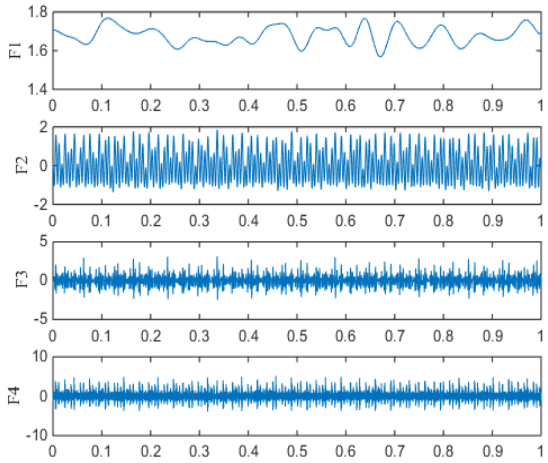

Fig. 4. Amplitude functions

According to the values of parameter (P) used to evaluate impulsivity (Table.5), the new vibration signal containing fault data can be reconstructed using the following formula:

$$x(t) = [F3_{AI}(t) + F4_{AI}(t)] \times cos\left(F4_{QI}(t)\right) \quad (30)$$

Table 5. Values of parameter (P)

Functions	Phase (QI)	Amplitude (AI)
F1	0.0398	0
F2	0.0559	0.0873
F3	0.1524	0.6253
F4	0.3003	3.0512

In the spectrum of absolute values (Fig.5) of the new signal filtered by the MHPO1 operator, we observe a high-amplitude peak at a frequency of 157.5 Hz. This value is very close to the fault frequency of the inner ring of bearing 6205-SKF (157.5 Hz ≈ 157.94 Hz). In this case, the faulty component is identified and located at the peak frequency.

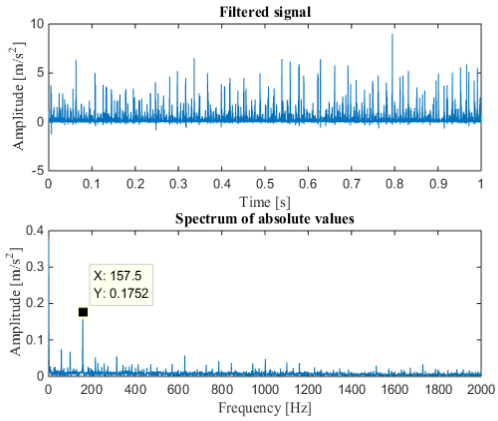

Fig. 5. Spectrum of absolute values

Case 2: Signal from the 6203-SKF bearing

The time and frequency domains of the vibration signal are shown in Fig. 6.

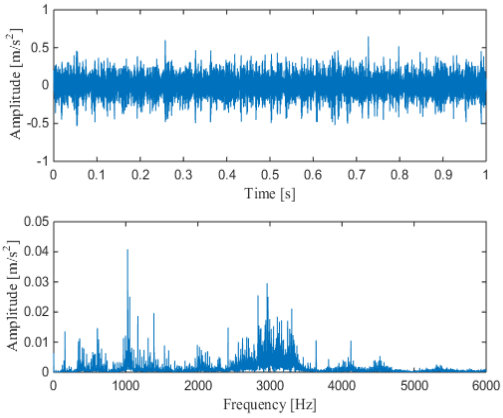

Fig. 6. Vibration signals in the time and frequency domains

The frequency domain, or signal spectrum, show several peaks at different frequencies, making fault detection impossible because of the shape complexity. To this end, we apply the proposed method to simplify the shape. The results of this method are summarized as follows:

- The amplitude (AI) and phase (QI) of the signal are illustrated in Fig. 7, and the values of parameter (P) for the four functions obtained by the EFD method are shown in Table 6. According to parameter (P), the new vibration signal, which contains data dependent on defects, is expressed as follows:

$$\begin{cases} AI_n(t) = F3_{AI}(t) + F4_{AI}(t) \\ QI_n(t) = F3_{QI}(t) + F4_{QI}(t) \end{cases} \quad (31)$$

$$x(t) = AI_n(t) \times cos(QI_n(t)) \quad (32)$$

Table 6. Parameter (P) values of the 6203 bearing signal

Functions	Phase (QI)	Amplitude (AI)
F1	0.0382	0
F2	0.0855	0.0705
F3	0.2864	0.3322
F4	0.2693	0.3562

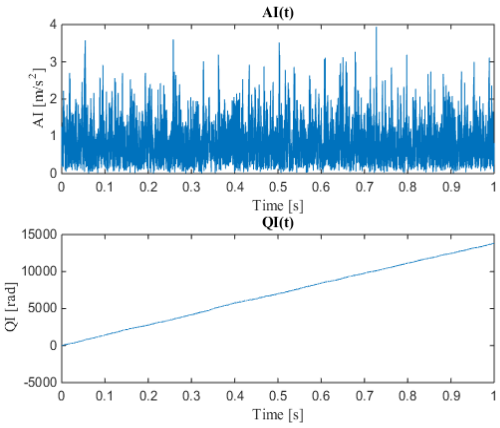

Fig. 7. Signal amplitude and phase of bearing 6203

- The absolute value spectrum of the new filtered signal (Fig.8) illustrates a high-amplitude peak at the fault frequency of the inner ring of bearing 6203-SKF (142.63 Hz≈142.1 Hz).

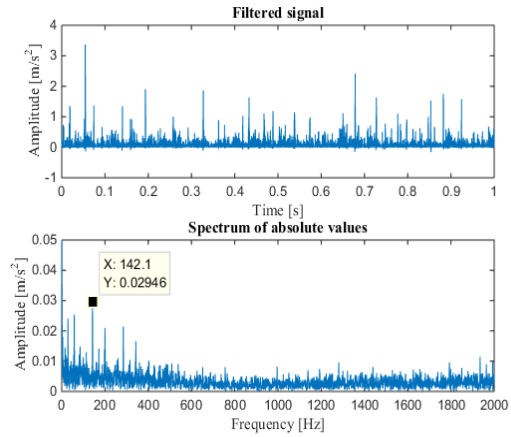

Fig. 8. Absolute value spectrum of the 6203 bearing signal

3.2. Ottawa university database

The vibration signals in this database were collected using a test strip consisting of a single-phase electric motor operating at a constant speed of 1750 rpm [28]. The motor shaft is supported by model 6203 ZZ ball bearings, and vibrations from these bearings are collected by a model PCB 623C01 accelerometer mounted by a magnet on the bearing housing [28]. Vibration signal data were connected between the computer and sensor via a data acquisition system and recorded as MATLAB files with a sampling frequency of 42 kHz [28]. In addition, signals related to inner ring, outer ring, and cage faults were recorded under a load of 400 N, but no load was applied to signals related to ball faults [28].

We analyzed the fault signal of the outer ring of the NSK 6203 ZZ bearing according to Eq. (33) [11] and the parameters in Table 7 [28]. The fault frequency of the outer ring is 88.95 Hz.

$$F_{or} = \frac{z \times Fr}{2}\left(1 - \frac{d}{Dm}\cos(a)\right) \tag{33}$$

Table 7. Parameters of the NSK 6203 ZZ bearing

Pitch diameter	28.5 mm
Ball diameter	6.77 mm
Number of balls	8

3.2.1. Discussions and results

On the basis of the EFD method decomposition of the signal amplitude and phase into four functions (F), the impulsivity of each function is evaluated by parameter (P). Then, on the basis of the values of parameter (P), the new signal is reformulated as defined by Eqs. (24 and 25). The main results are illustrated as follows:

- The new vibration signal is expressed as follows:

$$\begin{cases} AI_n(t) = \sum_{i=2}^{4} F_i(t) \\ QI_n(t) = F_4(t) \\ x(t) = AI_n(t) \times cos(QI_n(t)) \end{cases} \tag{34}$$

Table 8. Evaluation of impulsivity by parameter (P)

Functions	Phase (QI)	Amplitude (AI)
F1	0.0299	0
F2	0.1537	0.4313
F3	0.1558	0.3634
F4	0.5752	2.7055

- The spectrum of the absolute values of the filtered signal reveals a high amplitude peak at the outer ring fault frequency (88.44 Hz ≈ 88.95 Hz), as shown in Figure 9. Thus, the fault is identified at the frequency of the peak.

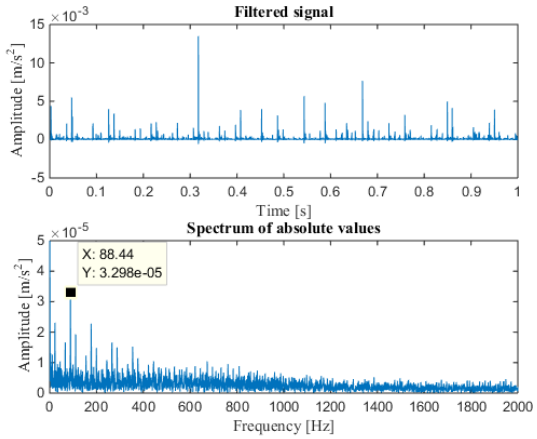

Fig. 9. Spectrum of the absolute values of the filtered signal

4. DETECTION METHOD COMPARISONS

Several diagnostic methods exist, but the most popular and widely used are envelope analysis and the deconvolution method. The envelope analysis consists of two steps [29]:

- Step 1: Filtering the vibration signal using a band-pass filter centered on the resonance frequency. This frequency is determined using methods such as Kurtogram and Autogram.
- Step 2: Determination of the envelope spectrum using the Fourier and Hilbert transforms, as

described in equations (3) and (35). Next, the fault is detected by analyzing the peak frequency.

$$AI(f) = \int_{-\infty}^{+\infty} AI(t)e^{-j2f\pi t}dt \qquad (35)$$

Thus, deconvolution methods such as MCKD are based on the extraction of signal pulses [11]. Then, a determination of the signal envelope spectrum obtained after the deconvolution operation is performed to detect the defect [11]. The steps of these methods are as follows [11]:

- Step 1: Deconvolution of the signal using the MCKD method.
- Step 2: Identify the envelope spectrum using equations (3) and (35).

The envelope analysis and fault detection approach using deconvolutions are applied to the outer ring vibration signal present in the University of Ottawa database, which was previously analyzed using the proposed method. Once the envelope analysis has been performed, a kurtogram of the signal illustrates a maximum value of spectral kurtosis (48.2), as shown in Figure (10). The two pass frequencies of the filter are 10500 Hz and 15750 Hz, with a resonant frequency of 13125 Hz and a bandwidth of 5250 Hz. Then, in the envelope spectrum, we find a significant peak at the fault frequency (88.44 Hz ≈ 88.95 Hz), as shown in Figure (11).

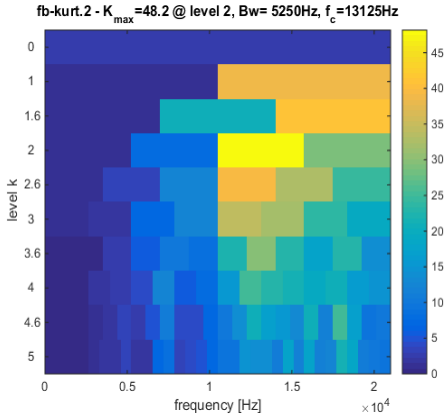

Fig. 10. Kurtogram

Thus, the envelope spectrum determined after extracting the signal pulses via the MCKD deconvolution method, with the following input parameters: filter length 100, order 2, period 300, and number of insertions 10, shows a peak at the fault frequency, as shown in Figure (12).

The proposed methods, envelope analysis, and deconvolution method give the same results, as shown in Figures (9, 11 and 12). This result is represented by a peak of high amplitude at the defect frequency. However, the amplitude values differ: $3.29 \times 10^{-5}\ m/s^2$ for the proposed method, $0.001\ m/s^2$ for the envelope analysis, and $0.01\ m/s^2$ for the deconvolution method.

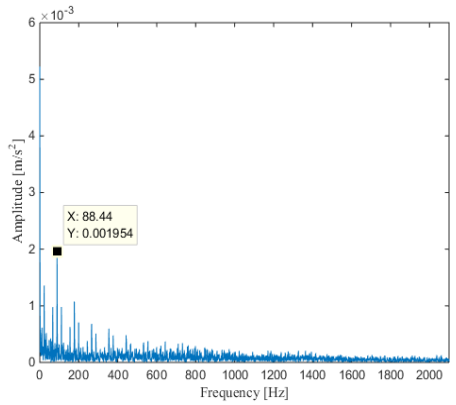

Fig. 11. Result of the envelope analysis

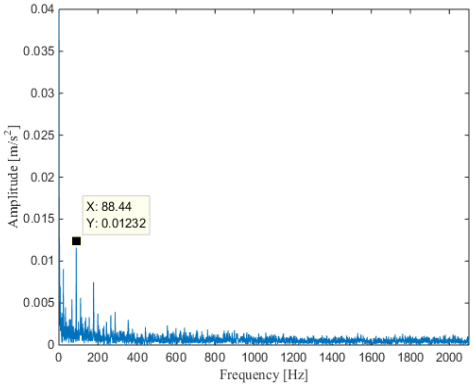

Fig. 12. Result of the deconvolution method

4.1. Influence of decomposition level

The proposed method involves two parameters: the vibration signal and the number of functions to be decomposed using the EFD method. The effect of the number of functions on the final result is visualized according to the frequency of the peak present in the spectrum of absolute values, for each variation of the number of functions (F) between 2 and 5. After applying the proposed method to the vibration signal for a variation in the number of functions from 2 to 5, the new vibration signals are shown in Table (9).

In the spectrum of absolute values of each new signal, decomposition levels 2, 3, 4 and 5 show better results. This is illustrated in Figures (13 and 14). Increasing the decomposition levels from five, such as 6 and 10, shows the same results, indicating that the decomposition level has no influence.

Table 9. New vibration signals

Decomposition level	New signals
2	$\begin{cases} AI_n(t) = F_2(t) \\ QI_n(t) = F_2(t) \\ x(t) = AI_n(t) \times cos(QI_n(t)) \end{cases}$
3	$\begin{cases} AI_n(t) = F_2(t) + F_3(t) \\ QI_n(t) = F_3(t) \\ x(t) = AI_n(t) \times cos(QI_n(t)) \end{cases}$

4	$\begin{cases} AI_n(t) = F_2(t) + F_3(t) + F_4(t) \\ QI_n(t) = F_4(t) \\ x(t) = AI_n(t) \times cos(QI_n(t)) \end{cases}$
5	$\begin{cases} AI_n(t) = F_4(t) + F_5(t) \\ QI_n(t) = F_4(t) + F_5(t) \\ x(t) = AI_n(t) \times cos(QI_n(t)) \end{cases}$

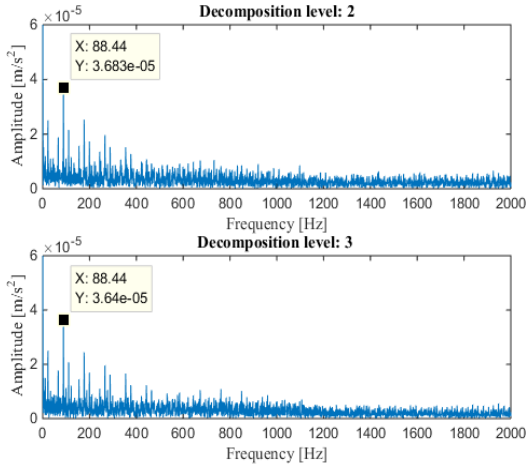

Fig. 13. Absolute value spectrum for levels 2 and 3

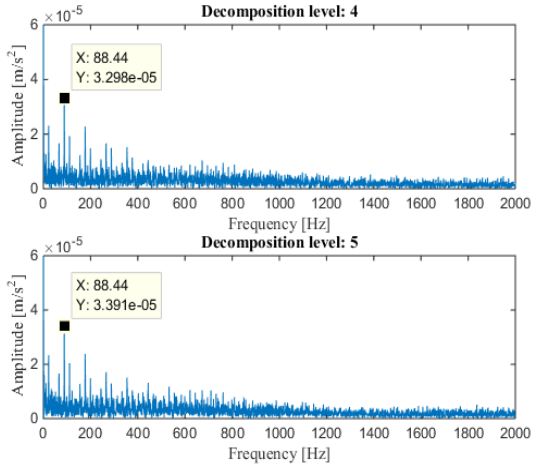

Fig. 14. Absolute value spectrum for levels 4 and 5

5. CONCLUSION

Following analysis of the vibration signals related to bearing faults, which are available in two separate databases, we can deduce that the spectrum of the original vibration signal is complex because of noise and the combination of useful and useless data. To obtain useful data, it is necessary to apply appropriate processing based on the evaluation of the impulsivity created by defects in the signals using parameters. In addition, evaluating the impulsivity of the instantaneous amplitude and instantaneous phase of the signal offers an excellent opportunity to reconstruct a new vibration signal containing information about the defects.

There is a difference between the parameters used to measure the pulse, and each parameter can have a threshold to define whether the bearing is in a failed or healthy state. Due to several thresholds, there are differences in the selection of effective functions (F), determined by the EFD method. To avoid this difference, we propose a parameter (P) considered as a product between all parameters. Finally, we obtain a single important threshold that facilitates the reconstruction of an effective signal.

The spectrum of absolute values enables faults to be detected simply and efficiently, based on peak frequency. It can be used as the final diagnostic step.

Source of funding: *This research received no external funding.*

Author contributions: *research concept and design, K.M., Y.M., D.K.; Collection and/or assembly of data, K.M., Y.M., D.K.; Data analysis and interpretation, K.M., Y.M., D.K.; Writing the article, K.M., Y.M., D.K.; Critical revision of the article, K.M., Y.M., D.K.; Final approval of the article, K.M., Y.M., D.K.*

Declaration of competing interest: *The authors declare that they have no known competing financial interests or personal relationships that could have appeared to influence the work reported in this paper.*

REFERENCES

1. Gundewar SK, Prasad VK. Condition monitoring and fault diagnosis of induction motor. Journal of Vibration Engineering & Technologies 2021; 9: 643-674. https://doi.org/10.1007/s42417-020-00253-y.
2. Du Y. Damage detection techniques for wind turbine blades: A review. Mechanical Systems and Signal Processing 2020; 141: 106445. https://doi.org/10.1016/j.ymssp.2019.106445.
3. Ghazali M, Hazwan M, Rahiman W. Vibration analysis for machine monitoring and diagnosis: a systematic review. Shock and Vibration 2021; 1-25. https://doi.org/10.1155/2021/9469318.
4. Bouaouiche K, Menasria Y, Khalfa D. Diagnosis of rotating machine defects by vibration analysis. Acta IMEKO 2023; 12(1): 1-6. https://doi.org/10.21014/actaimeko.v12i1.1438.
5. Dyer D, Stewart RM. Detection of rolling element bearing damage by statistical vibration analysis. (1978): 229-235. https://doi.org/10.1115/1.3453905.
6. Albezzawy MN, Nassef MG, Sawalhi N. Rolling element bearing fault identification using a novel three-step adaptive and automated filtration scheme based on Gini index. ISA transactions 2020; 101: 453-460. https://doi.org/10.1016/j.isatra.2020.01.019.
7. Xiaodong J. A geometrical investigation on the generalized lp/lq norm for blind deconvolution. Signal Processing 2017; 134: 63-69. https://doi.org/10.1016/j.sigpro.2016.11.018.
8. Zhao M. Feature mining and health assessment for gearboxes using run-up/coast-down signals. Sensors 2016; 16(11): 1837. https://doi.org/10.3390/s16111837.
9. Bingchang H. A comparison of machine health indicators based on the impulsiveness of vibration signals. Acoustics Australia 2021; 49: 199-206. https://doi.org/10.1007/s40857-021-00224-7.

10. Ziwei Z. Bearing fault diagnosis via generalized logarithm sparse regularization. Mechanical Systems and Signal Processing 2022; 167: 108576. https://doi.org/10.1016/j.ymssp.2021.108576.
11. Bouaouiche K. Yamina M, Dalila K. Detection and diagnosis of bearing defects using vibration signal processing. Archive of Mechanical Engineering 2023; 70(3):433–452. https://doi.org/10.24425/ame.2023.146849.
12. Bouaouiche K. Menasria Y, Dalila K. Detection of defects in a bearing by analysis of vibration signals. Diagnostyka 2023; 24(2). http://dx.doi.org/10.29354/diag/162230.
13. Jain, PH, Bhosle SP. A review on vibration signal analysis techniques used for detection of rolling element bearing defects. SSRG Int. J. Mech. Eng 2021; 8: 14-29. https://doi.org/10.14445/23488360/IJME-V8I1P103.
14. Huang NE. Review of empirical mode decomposition. Wavelet Applications VIII. 2001; 4391. https://doi.org/10.1117/12.421232.
15. Nazari M, Sakhaei SM. Successive variational mode decomposition. Signal Processing 2020; 174: 107610. https://doi.org/10.1016/j.sigpro.2020.107610.
16. Peng B. A survey on fault diagnosis of rolling bearings. Algorithms 2022; 15(10): 347. https://doi.org/10.3390/a15100347.
17. Yongjian S, Li S. Bearing fault diagnosis based on optimal convolution neural network. Measurement 2022; 190: 110702. https://doi.org/10.1016/j.measurement.2022.110702.
18. Zuo L. A multi-layer spiking neural network-based approach to bearing fault diagnosis. Reliability Engineering & System Safety 2002;225:: 108561. https://doi.org/10.1016/j.ress.2022.108561.
19. Altaf M. A new statistical features based approach for bearing fault diagnosis using vibration signals. Sensors 2022; 22(5): 2012. https://doi.org/10.3390/s22052012.
20. Feldman M. Hilbert transform in vibration analysis. Mechanical systems and signal processing 2011; 25(3): 735-802. https://doi.org/10.1016/j.ymssp.2010.07.018.
21. Zhou W. Empirical fourier decomposition. arXiv preprint arXiv 2019; 1912.00414. https://doi.org/10.48550/arXiv.1912.00414.
22. Yonghao M, Zhao M, Hua J. Research on sparsity indexes for fault diagnosis of rotating machinery. Measurement 2020; 158: 107733. https://doi.org/10.1016/j.measurement.2020.107733.
23. Hebda-Sobkowicz J, Zimroz R, Wyłomańska A. Selection of the Informative Frequency Band in a Bearing Fault Diagnosis in the Presence of Non-Gaussian Noise—Comparison of Recently Developed Methods. Applied Sciences 2020; 10(8): 2657. https://doi.org/10.3390/app10082657.
24. Case Western Reserve University bearing database. https://engineering.case.edu/bearingdatacenter
25. Bingyan C. A performance enhanced time-varying morphological filtering method for bearing fault diagnosis. Measurement 2021; 176: 109163. https://doi.org/10.1016/j.measurement.2021.109163.
26. Yifan L, Liang X, Zuo MJ. Diagonal slice spectrum assisted optimal scale morphological filter for rolling element bearing fault diagnosis. Mechanical Systems and Signal Processing 2017; 85: 146-161. https://doi.org/10.1016/j.ymssp.2016.08.019.
27. Yifan L, Liang X, Zuo MJ. A new strategy of using a time-varying structure element for mathematical morphological filtering. Measurement 2017; 106: 53-65. https://doi.org/10.1016/j.measurement.2017.04.032.
28. Mert S, Dumond P, Bouchard M. University of Ottawa constant load and speed rolling-element bearing vibration and acoustic fault signature datasets. Data in Brief 2023; 109327. https://doi.org/10.1016/j.dib.2023.109327.
29. Tse PW, Peng YH, Yam R. Wavelet analysis and envelope detection for rolling element bearing fault diagnosis—their effectiveness and flexibilities. J. Vib. Acoust. 2001; 123(3): 303-310. https://doi.org/10.1115/1.1379745.

BOUAOUICHE Karim, PhD student at Badji Mokhtar-Annaba University, faculty of technology, department of electromechanics. His current research concerns the detection of bearing faults using vibration signal analysis. e-mail: karimbouaouiche@gmail.com

Yamina MENASRIA, Lecturer at Badji Mokhtar University in Annaba, Faculty of Technology, Department of Electromechanics, and director of the thesis entitled "Detection of Bearing Faults by Vibration Signal Analysis."
e-mail: y.menasria.dpt.elm@gmail.com

Dalila KHALFA, Lecturer at Badji Mokhtar University in Annaba, Faculty of Technology, Department of Electromechanics, co-director of the thesis entitled "Detection of Bearing Faults by Vibration Signal Analysis."
e-mail: maint_dal@yahoo.fr